Desalination and Water Treatment
www.deswater.com

doi: 10.5004/dwt.2018.21856

104 (2018) 315–323
February

Modeling and optimization of decolorization of C.I. Reactive Orange 16 via $SO_4^{\bullet-}$ radicals by response surface methodology

Ozlem Esen Kartal

Department of Chemical Engineering, Inonu University, Malatya 44280, Turkey, Tel. +90 422 3774751; Fax: +90 422 3410046; email: ozlem.kartal@inonu.edu.tr

Received 23 March 2017; Accepted 25 December 2017

ABSTRACT

Modeling and optimization of decolorization of C.I. Reactive Orange 16 (RO16) via $SO_4^{\bullet-}$ by response surface methodology (RSM) have been investigated. $SO_4^{\bullet-}$ was generated in situ by activation of persulfate via UV irradiation. Planning of experimental runs was made by central composite design technique of RSM. A 2^4 full factorial design was applied to evaluate the interactive effects of process variables of $Na_2S_2O_8$ dosage (X_1, g L^{-1}), initial dye concentration (X_2, mg L^{-1}), temperature (X_3, °C) and time (X_4, min) on decolorization efficiency considered as response (Y). A second-order model for decolorization of RO16 was obtained and the experimental results fitted the model predictions well. The optimum reaction conditions to obtain maximum decolorization efficiency was found as $Na_2S_2O_8$ dosage of 1.60 g L^{-1}, dye concentration of 31 ppm, temperature of 33°C and time of 66 min. Quenching studies showed that the main reactive radical was $SO_4^{\bullet-}$. The second-order reaction rate constant between $SO_4^{\bullet-}$ and RO16 was found to be 1.36×10^9 M^{-1} s^{-1}.

Keywords: Reactive Orange 16; Sulfate radical; RSM; Decolorization; Optimization; Competition kinetics

1. Introduction

Textile industry generates large volumes of wastewater due to consumption of nearly 21–377 m^3 of water per ton of textile product. Besides a considerable amount and a variety of chemicals which are mainly inorganic salts and dyes are used during bleaching, dyeing or finishing processes of textile industry. Consequently, textile industry is considered as one of the most polluting industry with relatively high COD and low BOD values [1]. Reactive dyes are widely used in cotton dyeing process of textile industry because of their high washing fastness, bright colors and simple application procedure. The fixation efficiency of reactive dyes is between 50% and 80%, resulting in the presence of 20% and 50% of unfixed dye in textile wastewater [2]. Discharge of colored wastewater to receiving water bodies even at small concentrations (1 mg L^{-1}) causes non-aesthetic pollution and eutrophication [1,3,4]. In view of prevention of water pollution, remediation of wastewater originating from textile industry is of basic significance. Environmental considerations deeply involve the use of efficient treatment technologies to remove contaminants from textile wastewaters to meet stringent discharge limits. Physical, chemical and biological methods have been considered for the remediation of textile wastewaters so far, but they do not always provide efficient and economical results [5–8]. Physical methods are non-destructive and involve further treatments. Biological methods are found to be inefficient to decompose poorly biodegradable contaminants [9–12]. In recent years, sulfate radical ($SO_4^{\bullet-}$) based chemical treatment technology has emerged as an alternative to established technologies. It seems reasonable to consider $SO_4^{\bullet-}$ to oxidize water contaminants since it is a strong oxidant with a high standard redox potential between 2.6 and 3.1 V [13–17]. Azo dyes are characterized by the presence of –N=N– azo bond linking aromatic rings. They contribute to the largest groups of reactive dyes used to dye cotton, wool and polyamide fibers in textile industry. They are considered as non-biodegradable contaminants due to their complicated and stable chemical structure. Therefore, applicability of $SO_4^{\bullet-}$ based technology for degradation of azo dyes is an important approach to prevent water pollution.

$SO_4^{\bullet-}$ can be generated in situ by activation of persulfate ($S_2O_8^{2-}$, PS) or peroxymonosulfate (HSO_5^-, PMS) via thermal, chemical or UV irradiation methods [18,19]. Reactions related with these methods are given in Table 1. Once $SO_4^{\bullet-}$ is generated, organic contaminants (R) are degraded through radical chain reactions given in Eqs. (1)–(4) [23].

$$SO_4^{\bullet-} + RH_2 \rightarrow SO_4^{2-} + H^+ + RH^{\bullet} \quad (1)$$

$$RH^{\bullet} + S_2O_8^{2-} \rightarrow R + SO_4^{2-} + H^+ + SO_4^{\bullet-} \quad (2)$$

$$SO_4^{\bullet-} + RH \rightarrow R^{\bullet} + SO_4^{2-} + H^+ \quad (3)$$

$$2R^{\bullet} \rightarrow RR \quad (4)$$

In addition to activation of PS or PMS via thermal, chemical or UV irradiation methods, recently a novel method based on activation of sulfite with iron-based compounds has been reported to generate $SO_4^{\bullet-}$. Fe(II)-sulfite [25], photo-Fe(II)-sulfite [26–28] Fe^0-sulfite [29], heterogeneous $CoFe_2O_4$-S(IV)-O_2 [30] systems were investigated in the literature.

In an attempt to investigate and optimize process variables that affect the degradation or decolorization of azo dyes, experimental design methodology should be applied. Classical optimization methods involve 'one factor at a time' approach to study the effect of parameters. In these methods, a large number of experiments are required and interactive effect of variables cannot be examined. Response surface methodology (RSM), one of the experimental design methods, is a statistical tool for modeling and optimization of processes by considering individual and interactive effects of variables on response of interest with a reduced number of experimental runs [31].

In this study, decolorization of C.I. Reactive Orange 16 (RO16), chosen as a model water contaminant, was investigated via $SO_4^{\bullet-}$ based process. RSM was employed to determine the effects of sodium peroxidisulfate ($Na_2S_2O_8$) dosage, initial dye concentration, temperature and time individually and interactively upon response, that is, decolorization efficiency. Besides, a model equation was established and optimization of decolorization of RO16 was conducted. Under optimized conditions, decolorization of synthetic dye-bath effluent was also examined.

2. Experimental

2.1. Materials

Unless otherwise stated, all chemicals were of analytical grade and used without further purification. $Na_2S_2O_8$ (≥99.9%), *tert*-butyl alcohol (TBA, 99%) and HCl (37% w/w) were purchased from Merck. NaOH and ethanol (EtOH, absolute ≥99.8%) were purchased from Sigma-Aldrich. Phenol (Ph, 99.5%) was purchased from Carlo Erba. A commercially available RO16 from DyStar was used as received and its properties are given in Table 2.

2.2. Experimental procedure

A cylindrical batch photoreactor with a water jacket was used for decolorization of RO16. The temperature of a reaction medium was adjusted by circulating water that was heated in the thermostated water bath (Nüve BS 302) through the water jacket of the photoreactor. Irradiation was provided with two 8 W UV-C lamps of (Philips) with a wavelength of 254 nm placed around the photoreactor. Aqueous RO16 solution (500 mL) at desired concentration prepared by diluting stock solution was put into photoreactor and stirred for 10 min under dark conditions. Then, $Na_2S_2O_8$ at appropriate

Table 2
Characteristics of C.I. Reactive Orange 16

Structure	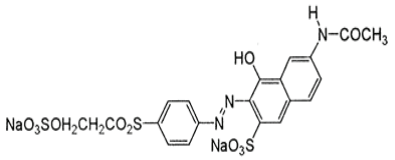
IUPAC name	Disodium 6-acetamido-4-hydroxy-3-[(*E*)-(4-{[2-(sulfonatooxy) ethyl] sulfonyl}phenyl)diazenyl]-2-naphthalenesulfonate
Chemical formula	$C_{20}H_{17}N_3Na_2O_{11}S_3$
Molecular weight	617.54
λ_{max}, nm	493
Color index	17,757

Table 1
Activation methods of persulfate ($S_2O_8^{2-}$) and peroxymonosulfate (HSO_5^-)

Activation	Equation	Contaminant	Reference
Thermal	$S_2O_8^{2-} \rightarrow 2SO_4^{\bullet-}$	Bisoprolol	[20]
	$HSO_5^- \rightarrow OH^{\bullet} + SO_4^{\bullet-}$	Microcystin-LR	[21]
Chemical	$S_2O_8^{2-} + Ag^+ \rightarrow Ag^{2+} + SO_4^{\bullet-} + SO_4^{2-}$	2,4-Dichlorophenol	[22]
	$HSO_5^- + Co^{2+} \rightarrow Co^{3+} + SO_4^{\bullet-} + OH^-$		
UV irradiation	$S_2O_8^{2-} \rightarrow 2SO_4^{\bullet-}$	Basic Yellow 2	[23]
	$HSO_5^- \rightarrow OH^{\bullet-} + SO_4^{\bullet-}$	Ciprofloxacin	[24]

amount was added to dye solution. The pH of the solution was adjusted using either dilute NaOH or HCl solutions and measured by a digital pH-meter (Hanna pH-221). Finally, reaction was initiated by switching on UV-C lamps. The reaction mixture was stirred by magnetic stirrer (IKA RH KT/C) during the experiments. At a regular time intervals, samples were taken from the reaction medium to monitor decolorization of RO16 spectrophotometrically.

2.3. Analysis

RO16 concentration in the reaction medium was determined at maximum wavelength of 493 nm by means of a double beam Shimadzu UV-1700 Pharmaspec UV-Visible Spectrophotometer. The decolorization efficiency of the samples was calculated as follows (Eq. (5)) [32]:

$$\text{Decolorization}(\%) = \frac{C_0 - C}{C_0} \times 100 \quad (5)$$

where C_0 and C are the initial and treated dye concentrations, respectively.

Phenol concentration was determined using Agilent 1100 Series HPLC equipped with a C18 250 × 4.6 mm column and a diode array detector at a wavelength of 274 nm. The mobile phase was 20% acetonitrile and 80% water. The flow rate and injection volume were mL min^{-1} and 20 μL, respectively.

2.4. Experimental design approach

In this study, RSM was applied for modeling and optimization of decolorization of RO16 via $SO_4^{\bullet-}$ based process. Central composite design (CCD) technique of RSM is based on factorial design and consists of factorial (–1, +1), axial (0, ±α) and central points (0, 0). In this study, the planning of experimental runs was made by using CCD and a 2^4 full factorial design was applied with six replicates at the center point. $Na_2S_2O_8$ dosage (X_1, g L^{-1}), initial dye concentration (X_2, mg L^{-1}), temperature (X_3, °C) and time (X_4, min) were selected as independent variables with five levels (–α, –1, 0, 1, +α). The expression of $2^n + 2n + 6$ results in total 30 experimental runs for four independent variables (n). Decolorization efficiency given by Eq. (5) was considered as response (Y). Independent variables with their coded levels are given in Table 3.

Modeling and optimization of decolorization of RO16 via $SO_4^{\bullet-}$ by RSM were performed using trial version of Design Expert software (Version 10, Stat-Ease Inc., Minneapolis, USA). The relationship between coded independent variables (x_1, x_2, x_3, x_4) and response is given by a quadratic model equation (Eq. (6)).

$$\begin{aligned} Y = {} & b_0 + b_1x_1 + b_2x_2 + b_3x_3 + b_4x_4 + b_{12}x_1x_2 + b_{13}x_1x_3 \\ & + b_{14}x_1x_4 + b_{23}x_2x_3 + b_{24}x_2x_4 + b_{34}x_3x_4 + b_{11}x_1^2 \\ & + b_{22}x_2^2 + b_{33}x_3^2 + b_{44}x_4^2 \end{aligned} \quad (6)$$

In this equation, b_0 is a constant, b_1, b_2, b_3, b_4 are linear, b_{12}, b_{13}, b_{14}, b_{23}, b_{24}, b_{34} are interaction and b_{11}, b_{22}, b_{33}, b_{44} are quadratic term coefficients.

Table 3
Independent variables with their coded levels

Independent variables	Assigned levels and ranges of variables				
	–α	–1	0	1	+α
A: $Na_2S_2O_8$ dosage (X_1, g L^{-1})	0.1	0.9	1.7	2.5	3.3
B: Initial dye concentration (X_2, mg L^{-1})	5	20	35	50	65
C: Temperature (X_3, °C)	20	30	40	50	60
D: Time (X_4, min)	10	30	50	70	90

$\alpha = (2^n)^{1/4} = 2$

3. Results and discussion

3.1. Response surface modeling

The first step in CCD is conducting the experimental runs with determined independent variables by considering their levels. Then, coefficients of the model equation are predicted to establish the model equation in order to estimate response. Later, significance and adequacy of model are tested by analysis of variance (ANOVA) results. Accordingly, in this study, experimental runs were conducted by considering experimental design matrix with four factors of five levels given in Table 4. The quadratic model equation giving an empirical relationship between decolorization efficiency and independent variables in coded values was obtained by multiple regression analysis on experimental data (Eq. (7)).

$$\begin{aligned} Y = {} & 95.30 + 11.00x_1 - 9.01x_2 + 0.81x_3 + 6.61x_4 + 6.14x_1x_2 \\ & + 0.21x_1x_3 - 3.17x_1x_4 + 0.43x_2x_3 + 3.54x_2x_4 - 0.38x_3x_4 \\ & - 7.60x_1^2 - 1.63x_2^2 + 1.81x_3^2 - 2.31x_4^2 \end{aligned} \quad (7)$$

Table 5 reveals the ANOVA results of model. Statistical significance of the model can be evaluated by Fisher's F test (F value) or probability value (p value, Prob. > F) with 95% confidence level. The model F value of 6.08 confirmed that the model was significant for RO16 decolorization and there was only 0.06% chance that a model F value could occur due to noise. The calculated p value less than 0.05 indicated that model terms were significant. In this study, p values implied that $Na_2S_2O_8$ dosage (A), initial dye concentration (B) and time (D) had highly significant linear effects on decolorization efficiency. Considering interactive and quadratic effects of variables, interaction between $Na_2S_2O_8$ dosage and initial dye concentration (AB) and quadratic effect of $Na_2S_2O_8$ dosage (A^2) were significant according to their corresponding p values.

The experimental vs. predicted decolorization efficiency values are shown in Fig. 1. Experimental values were obtained by measuring response in experimental runs, while predicted values were estimated by using model equation. As can be seen from Fig. 1, model equation sufficiently predicted response. Coefficient of determination (R^2) value of model quantitatively indicates correlation between experimental

Table 4
Experimental design matrix with experimental and predicted response values

Run	X_1 (g L^{-1})	X_2 (mg L^{-1})	X_3 (°C)	X_4 (min)	x_1	x_2	x_3	x_4	Y (%) Experimental	Y (%) Predicted
1	0.9	20	30	30	–1	–1	–1	–1	95.42	82.91
2	2.5	20	30	30	+1	–1	–1	–1	97.86	98.55
3	0.9	50	30	30	–1	+1	–1	–1	50.60	44.69
4	2.5	50	30	30	+1	+1	–1	–1	88.57	84.89
5	0.9	20	50	30	–1	–1	+1	–1	94.80	84.02
6	2.5	20	50	30	+1	–1	+1	–1	99.22	100.50
7	0.9	50	50	30	–1	+1	+1	–1	54.58	47.51
8	2.5	50	50	30	+1	+1	+1	–1	92.02	88.55
9	0.9	20	30	70	–1	–1	–1	+1	99.03	96.14
10	2.5	20	30	70	+1	–1	–1	+1	99.60	99.12
11	0.9	50	30	70	–1	+1	–1	+1	80.91	72.07
12	2.5	50	30	70	+1	+1	–1	+1	95.18	99.60
13	0.9	20	50	70	–1	–1	+1	+1	99.61	95.73
14	2.5	20	50	70	+1	–1	+1	+1	100.00	99.55
15	0.9	50	50	70	–1	+1	+1	+1	80.41	73.36
16	2.5	50	50	70	+1	+1	+1	+1	96.78	101.74
17	0.1	35	40	50	–α	0	0	0	20.39	42.90
18	3.3	35	40	50	+α	0	0	0	95.51	86.92
19	1.7	5	40	50	0	–α	0	0	99.22	106.77
20	1.7	65	40	50	0	+α	0	0	64.38	70.74
21	1.7	35	20	50	0	0	–α	0	93.27	100.91
22	1.7	35	60	50	0	0	+α	0	97.88	104.15
23	1.7	35	40	10	0	0	0	–α	59.06	72.83
24	1.7	35	40	90	0	0	0	+α	99.10	99.25
25	1.7	35	40	50	0	0	0	0	94.20	95.30
26	1.7	35	40	50	0	0	0	0	95.98	95.30
27	1.7	35	40	50	0	0	0	0	94.71	95.30
28	1.7	35	40	50	0	0	0	0	95.87	95.30
29	1.7	35	40	50	0	0	0	0	95.08	95.30
30	1.7	35	40	50	0	0	0	0	95.94	95.30

and predicted response values. It is expected that R^2 value should be close to 1. In this study, R^2 value of model was obtained as 0.8502, denoting that 85.02% of variability in response, that is, decolorization efficiency can be explained by the model.

Figs. 2–4 reveal contour plots (2D) and response surfaces (3D) of the interactive effects of variables on response. These plots were obtained by Design Expert software to indicate the effects of any two variables with a numerous combinations, while keeping the other constants at their central level. Figs. 2(a) and (b) show the interactive effect of $Na_2S_2O_8$ dosage and initial dye concentration considered as main variables according to ANOVA results at 40°C and reaction time of 50 min. As is evident from Fig. 2, when $Na_2S_2O_8$ dosage is in the range of 1.4–2.5 g L^{-1} and at initial dye concentration below about 32 mg L^{-1}, 100% of decolorization efficiency was obtained. An increase in initial dye concentration beyond 32 mg L^{-1} resulted in a considerable decrease in decolorization efficiency at low $Na_2S_2O_8$ dosages. Decolorization efficiency increased with increasing $Na_2S_2O_8$ dosages and decreasing initial dye concentration. As $Na_2S_2O_8$ dosage increases, more $SO_4^{\bullet-}$ and $OH^{\bullet}$ are generated according to Eqs. (8) and (9), resulting in the improvement of efficiency [33]. $OH^{\bullet}$ is another strong oxidant with a standard redox potential of 2.8 V [34].

$$S_2O_8^{2-} \rightarrow 2SO_4^{\bullet-} \quad (8)$$

$$SO_4^{\bullet-} + H_2O \rightarrow H^+ + SO_4^{2-} + OH^{\bullet} \quad (9)$$

Figs. 3(a) and (b) illustrate the interactive effect of $Na_2S_2O_8$ dosage and temperature at initial dye concentration of 35 mg L^{-1} and reaction time of 50 min. The lines of contour plot (Fig. 3(a)) indicate that at low $Na_2S_2O_8$ dosage values, lower decolorization efficiency was obtained with all selected temperature range (30°C–50°C). However, decolorization efficiency increased upon increasing $Na_2S_2O_8$ dosage even at 30°C. These results revealed that $Na_2S_2O_8$ dosage has more pronounced effect than temperature on decolorization efficiency. The thermal activation of $S_2O_8^{2-}$ is achieved above 40°C and as expected increasing temperature resulted in generation of more SO_4^{-}, thus providing higher decolorization

Table 5
Analysis of variance (ANOVA) for selected model

Source	Sum of squares (SS)	Degrees of freedom (DF)	Mean square (MS)	*F* value	Prob. > *F*
Model	8,791.20	14	627.94	6.08	0.0006
A	2,906.42	1	2,906.42	28.14	0.0001
B	1,947.06	1	1,947.06	18.85	0.0006
C	15.80	1	15.80	0.15	0.7012
D	1,047.16	1	1,047.16	10.14	0.0062
AB	603.07	1	603.07	5.84	0.0289
AC	0.71	1	0.71	6.873×10^{-3}	0.9350
AD	160.47	1	160.47	1.55	0.2317
BC	2.90	1	2.90	0.028	0.8692
BD	200.01	1	200.01	1.94	0.1843
CD	2.32	1	2.32	0.022	0.8829
A^2	1,583.19	1	1,583.19	15.33	0.0104
B^2	73.31	1	73.31	0.71	0.4127
C^2	89.75	1	89.75	0.87	0.3660
D^2	146.98	1	146.98	1.42	0.2514
Residual	1,549.23	15	103.28		
Lack of fit	1,546.43	10	154.64	275.82	0.0001
Pure error	2.80	5	0.56		
Corrected total	10,340.43	29			

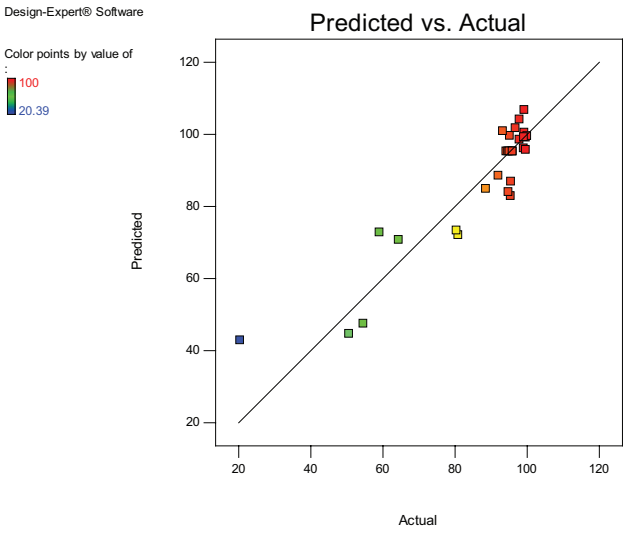

Fig. 1. The actual and predicted decolorization efficiency values.

efficiency [35]. In this study, activation of $S_2O_8^{2-}$ was provided by UV, therefore, thermal activation had no considerable effect.

Figs. 4(a) and (b) display the interactive effect of initial dye concentration and reaction time at $Na_2S_2O_8$ dosage of 1.7 g L^{-1} and temperature of 40°C. It can be seen that higher decolorization efficiency was obtained at low initial dye concentration values and long reaction times. As the initial dye concentration increases the solution becomes impermeable to UV radiation, yielding low decolorization efficiency [23].

3.2. Optimization

The optimization of decolorization of RO16 was performed using an optimization module in Design Expert software. Numerical optimization on the basis of desirability function was applied. The desired goal of response was set as maximize, while the goals of process variables were selected as in range. The goals transformed into desirability function which ranges between 0 and 1. Then, they are combined into an overall desirability function. The predicted optimum values are given by ramp plots. On the basis of the settings and highest desirability from the software, as shown in Fig. 5, the optimum values to maximize decolorization of RO16 were found as $Na_2S_2O_8$ dosage of 1.60 g L^{-1}, initial dye concentration of 31 ppm, temperature of 33°C and time of 66 min. Under these conditions the model resulted in 99.86% of decolorization efficiency of RO16. The optimum values were experimentally checked by conducting an experiment at optimum conditions and 98.5% of decolorization efficiency of RO16 was obtained. This result is in agreement with predicted response. Under optimized conditions, decolorization of synthetic dye-bath effluent was also investigated and as shown in Fig. 6, only 16% of decolorization efficiency of synthetic dye-bath effluent was achieved at 66 min of reaction time. As reaction time was further increased, an increase in decolorization efficiency was observed, reaching 64% at 300 min. However, almost complete decolorization was observed with RO16 solution at 66 min of reaction time. In dyeing process of textile industry, $NaCO_3$ and NaCl are used for stabilization of color. A low affinity of reactive dyes involves use of these salts in a large amount. Therefore, effluents from dyeing and washing processes are expected to contain a considerable amount of

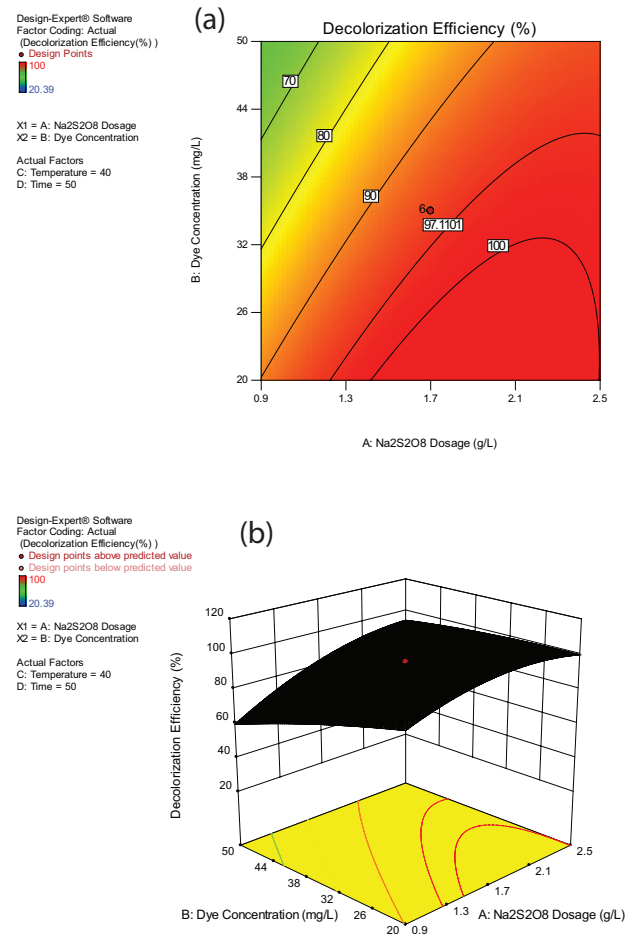

Fig. 2. Contour plot (a) and response surface (b) of the interactive effects of $Na_2S_2O_8$ dosage and initial dye concentration (other variables are held at zero level).

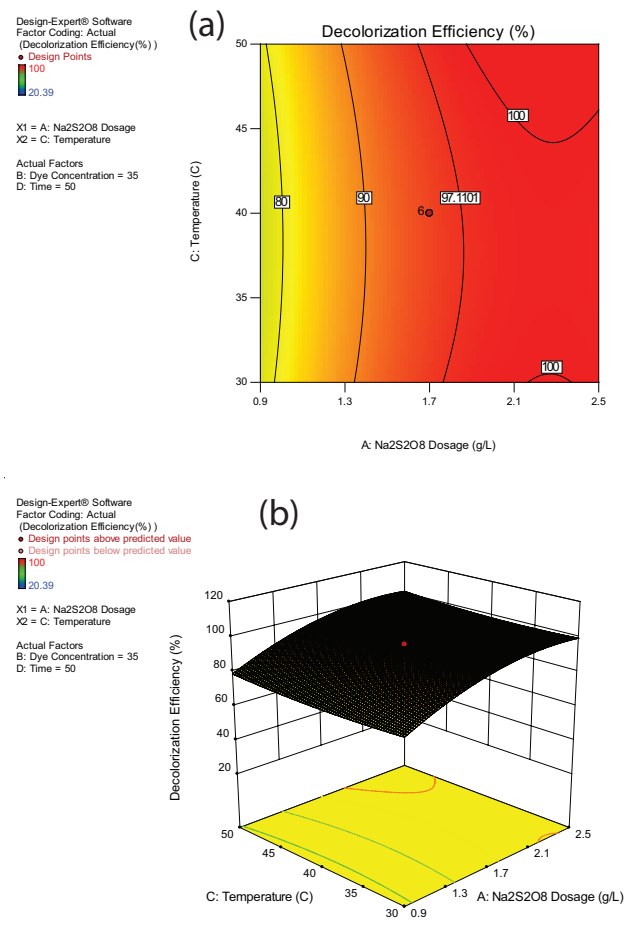

Fig. 3. Contour plot (a) and response surface (b) of the interactive effects of $Na_2S_2O_8$ dosage and temperature (other variables are held at zero level).

CO_3^{2-} and Cl^- [36,37]. Presence of a certain amount of CO_3^{2-} and Cl^- ions in synthetic dye-bath effluent caused to yield low decolorization efficiency.

3.3. Radical quenching studies

$OH^\bullet$ can be produced from $SO_4^{\bullet-}$ according to Eq. (9) in all pH values. Quenching studies were performed to investigate the contribution of $SO_4^{\bullet-}$ and $OH^\bullet$ by adding TBA and EtOH into reaction solution as a radical scavengers. Alcohol with a α-hydrogen (EtOH) reacts with these two radicals at high rates, while alcohol without a α-hydrogen (TBA) reacts faster with $OH^\bullet$ than $SO_4^{\bullet-}$ [38,39]. Accordingly, 0.672 M alcohol, corresponding to 100:1 molar ratio of alcohol vs. oxidant was introduced into reaction solution. As can be seen from Fig. 7, addition of TBA and EtOH resulted in decreasing decolorization efficiency from 98.5% to 91.1% and 34.9%, respectively. This indicates that $OH^\bullet$ was quenched upon addition of TBA and decolorization of RO16 was achieved by $SO_4^{\bullet-}$. However, in the presence of EtOH, decolorization efficiency of RO16 was considerably inhibited. These results suggest that $SO_4^{\bullet-}$ is the main reactive radical.

3.4. Degradation kinetics

The competition kinetic method was applied to determine the second-order reaction rate constant between $SO_4^{\bullet-}$ and RO16 using phenol as the competitor [40]. Since the predominate reactive radical is $SO_4^{\bullet-}$, kinetic expression can be written as:

$$-\frac{d[RO16]}{dt} = k_{RO16SO4^{\bullet-}}[RO16][SO_4^{\bullet-}] \quad (10)$$

where $k_{RO16SO4}^{\bullet-}$ is the second-order rate constant between $SO_4^{\bullet-}$ and RO16, $[SO_4^{\bullet-}]$ is the quasi-stationary concentration of $SO_4^{\bullet-}$ and [RO16] is the concentration of RO16 at time t. Similar equation can be written for phenol as:

$$-\frac{d[Ph]}{dt} = k_{PhSO4^{\bullet-}}[Ph][SO_4^{\bullet-}] \quad (11)$$

where $k_{PhSO4}^{\bullet-}$ is the second-order rate constant between $SO_4^{\bullet-}$ and phenol and [Ph] is the concentration of phenol at time t.

Eq. (12) is obtained by dividing Eq. (10) with Eq. (11):

$$\frac{\ln\left(\frac{[RO16]}{[RO16]_0}\right)}{\ln\left(\frac{[Ph]}{[Ph]_0}\right)} = \frac{k_{RO16SO4^{\bullet-}}}{k_{PhSO4^{\bullet-}}} \quad (12)$$

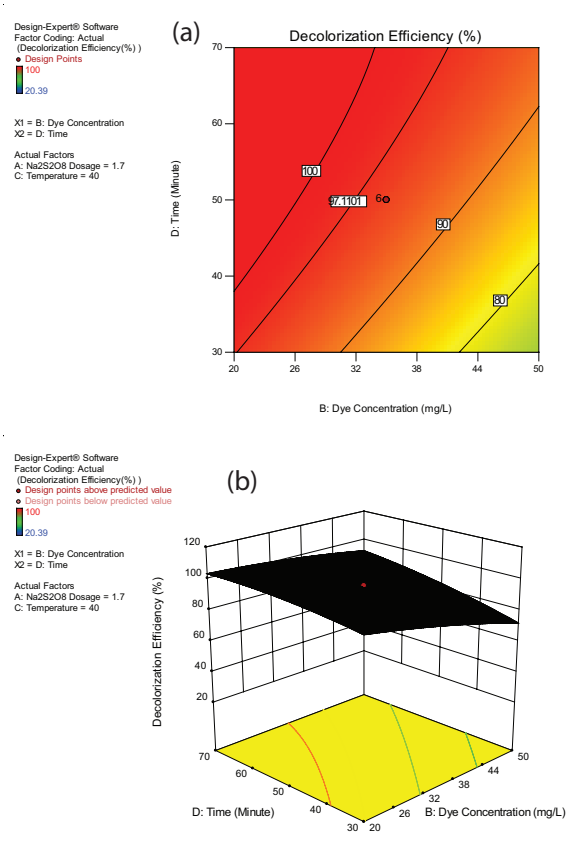

Fig. 4. Contour plot (a) and response surface (b) of the interactive effects of initial dye concentration and reaction time (other variables are held at zero level).

where $[RO16]_0$ and $[Ph]_0$ are initial concentrations of RO16 and phenol, respectively [25,41].

When $\ln\left(\frac{[RO16]}{[RO16]_0}\right)$ vs. $\ln\left(\frac{[Ph]}{[Ph]_0}\right)$ is plotted, a straight line with a slope of $\frac{k_{RO16SO4^{\bullet-}}}{k_{PhSO4^{\bullet-}}}$ is obtained. $k_{PhSO4}{}^{\bullet-}$ is given in literature as 8.8×10^9 M^{-1} s^{-1} [40]. According to Fig. 8, $k_{RO16SO4}{}^{\bullet-}$ was determined to be 1.36×10^9 M^{-1} s^{-1}. Zhou et al. [26] reported that the second-order reaction rate constant between $SO_4^{\bullet-}$ and Acid Orange 7 was determined as $6.80 \pm 0.68 \times 10^9$ M^{-1} s^{-1} by competition kinetics method in photo-iron(II) sulfite system.

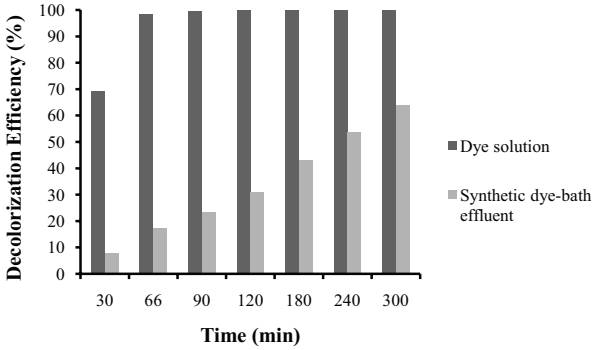

Fig. 6. Decolorization efficiency of RO16 dye solution and synthetic dye-bath effluent at optimum conditions.

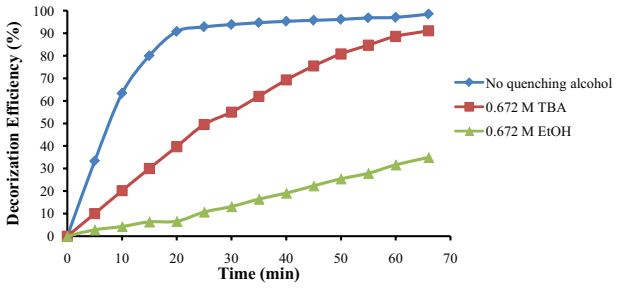

Fig. 7. Decolorization efficiency of RO16 at optimum conditions with and without radical scavengers.

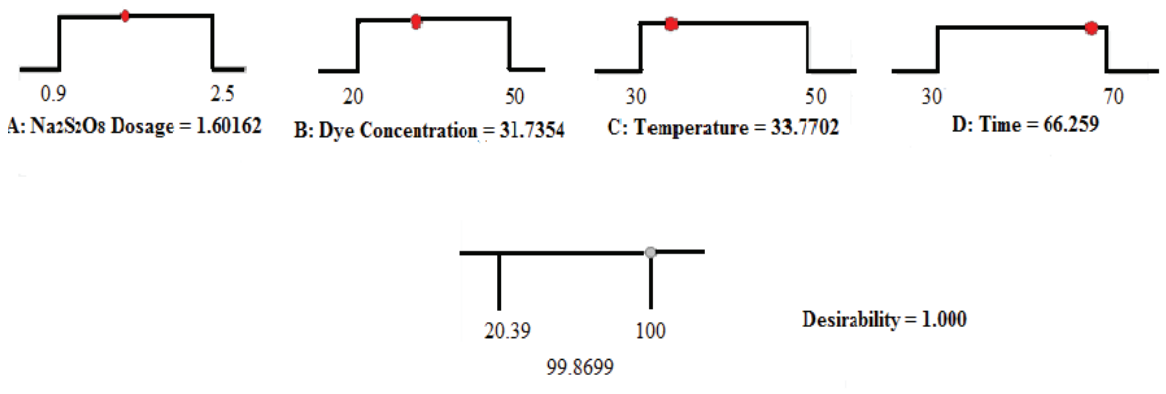

Fig. 5. Desirability ramp plots.

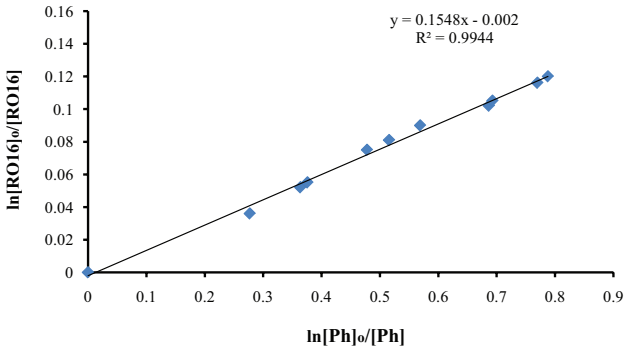

Fig. 8. $\ln[RO16]_0/[RO16]$ vs. $\ln[Ph]_0/[Ph]$ ($[Na_2S_2O_8]$ = 1.60 g L^{-1}, [RO16] = 31 mg L^{-1}, [Ph] = 31 mg L^{-1}, [TBA] = 0.672 M, T = 33°C).

4. Conclusions

In this study, decolorization of RO16 via $SO_4^{\bullet-}$ has been investigated. $SO_4^{\bullet-}$ was generated in situ by activation of persulfate via UV irradiation. Modeling and optimization of decolorization of RO16 were performed by RSM. A 2^4 full factorial CCD technique of RSM was successfully employed for experimental design and a quadratic model was developed with satisfactory degrees of fit. Numerical optimization on the basis of desirability function results reveal that the optimum values to maximize decolorization of RO16 were obtained as $Na_2S_2O_8$ dosage of 1.60 g L^{-1}, dye concentration of 31 ppm, temperature of 33°C and time of 66 min. Decolorization of synthetic dye-bath effluent of RO16 via $SO_4^{\bullet-}$ was evaluated and found that 64% of decolorization efficiency was achieved at 300 min. Quenching studies confirmed that the main reactive radical was $SO_4^{\bullet-}$ and the second-order reaction rate constant between $SO_4^{\bullet-}$ and RO16 was found to be 1.36×10^9 M^{-1} s^{-1} by competition kinetics method.

References

[1] A. Asghar, A.A.A. Raman, W.M.A.W. Daud, Advanced oxidation processes for in-situ production of hydrogen peroxide/hydroxyl radical for textile wastewater treatment: a review, J. Cleaner Prod., 87 (2015) 826–838.
[2] A. Khatri, M.H. Peerzada, M. Mohsin, M. White, A review on developments in dyeing cotton fabrics with reactive dyes for reducing effluent pollution, J. Cleaner Prod., 87 (2015) 50–57.
[3] P. Bansal, D. Sud, Photodegradation of commercial dye, Procion Blue HERD from real textile wastewater using nanocatalysts, Desalination, 267 (2011) 244–249.
[4] J. Wu, H. Doan, S. Upreti, Decolorization of aqueous textile reactive dye by ozone, Chem. Eng. J., 142 (2008) 156–160.
[5] T. Robinson, G. McMullan, R. Marchant, P. Nigam, Remediation of dyes in textile effluent: a critical review on current treatment technologies with a proposed alternative, Bioresour. Technol., 77 (2001) 247–255.
[6] Y. Anjaneyulu, N. Sreedhara Chary, D. Samuel Suman Raj, Decolorization of industrial effluents – available methods and emerging technologies – a review, Rev. Environ. Sci. Biotechnol., 4 (2005) 245–273.
[7] S. Mondal, Methods of dye removal from dye house effluent-an overview, Environ. Eng. Sci., 25 (2008) 383–396.
[8] K. Turhan, I. Durukan, S.A. Ozturkcan, Z. Turgut, Decolorization of textile basic dye in aqueous solution by ozone, Dyes Pigm., 92 (2012) 897–901.
[9] C.R. Holkar, A.J. Jadhav, D.V. Pinjari, N.M. Mahamuni, A.B. Pandit, A critical review on textile wastewater treatments: possible approaches, J. Environ. Manage., 182 (2016) 351–366.
[10] B. Panda, A survey on the present status of sustainable technologies for water pollutant abatement, Desal. Wat. Treat., 57 (2016) 28705–28714.
[11] P.A. Soares, R. Souza, J. Soler, T.F.C.V. Silva, S.M.A.G.U. Souza, R.A.R. Boaventura, V.J.P. Vilar, Remediation of a synthetic textile wastewater from polyester-cotton dyeing combining biological and photochemical oxidation processes, Sep. Purif. Technol., 172 (2017) 450–462.
[12] H. Eskandarloo, A. Badiei, C. Haug, Enhanced photocatalytic degradation of an azo textile dye by using TiO_2/NiO coupled nanoparticles: optimization of synthesis and operational key factors, Mater. Sci. Semicond. Process., 27 (2014) 240–253.
[13] K.C. Huang, R.A. Couttenye, G.E. Hoag, Kinetics of heat-assisted persulfate oxidation of methyl *tert*-butyl ether (MTBE), Chemosphere, 49 (2002) 413–420.
[14] J. Criquet, N. Karpel, V. Leitner, Degradation of acetic acid with sulfate radical generated by persulfate ions photolysis, Chemosphere, 77 (2009) 194–200.
[15] M.C. Yeber, L. Diaz, J. Fernandez, Catalytic activity of the $SO_4^{\bullet-}$ radical for photodegradation of the azo dye Cibacron Brilliant Yellow 3 and 3,4-dichlorophenol: optimization by application of response surface methodology, J. Photochem. Photobiol., A, 215 (2010) 90–95.
[16] S. Yang, P. Wang, X. Yang, L. Shan, W. Zhang, X. Shao, R. Niu, Degradation efficiencies of azo dye Acid Orange 7 by the interaction of heat, UV and anions with common oxidants: persulfate, peroxymonosulfate and hydrogen peroxide, J. Hazard. Mater., 179 (2010) 552–558.
[17] P. Hu, M. Long, Cobalt-catalyzed sulfate radical-based advanced oxidation: a review on heterogeneous catalysis and applications, Appl. Catal., B, 181 (2016) 103–117.
[18] J. Chen, L. Zhang, T. Huang, W. Li, Y. Wang, Z. Wang, Decolorization of azo dye by peroxymonosulfate activated by carbon nanotube: radical versus non-radical mechanism, J. Hazard. Mater., 320 (2016) 571–580.
[19] L. Ismail, C. Ferronato, L. Fine, F. Jaber, J.M. Chovelona, Elimination of sulfaclozine from water with $SO_4^{\bullet-}$ radicals: evaluation of different persulfate activation methods, Appl. Catal., B, 201 (2017) 573–581.
[20] A. Ghauch, A.M. Tuqan, Oxidation of bisoprolol in heated persulfate/H_2O systems: kinetics and products, Chem. Eng. J., 183 (2012) 162–171.
[21] M.G. Antoniou, A.A. de la Cruz, D.D. Dionysiou, Degradation of microcystin-LR using sulfate radicals generated through photolysis, thermolysis and e^- transfer mechanisms, Appl. Catal., B, 96 (2010) 290–298.
[22] G.P. Anipsitakis, D.D. Dionysiou, Radical generation by the interaction of transition metals with common oxidants, Environ. Sci. Technol., 38 (2004) 3705–3712.
[23] D. Salari, A. Niaeri, S. Aber, M.H. Rasoulifard, The photooxidative destruction of C.I. Basic Yellow 2 using UV/$S_2O_8^{2-}$ process in a rectangular continuous photoreactor, J. Hazard. Mater., 166 (2009) 61–66.
[24] M. Mahdi-Ahmed, S. Chiron, Ciprofloxacin oxidation by UV-C activated peroxymonosulfate in wastewater, J. Hazard. Mater., 265 (2014) 41–46.
[25] L. Chen, X. Peng, J. Liu, J. Li, F. Wu, Decolorization of Orange II in aqueous solution by an Fe(II)/sulfite system: replacement of persulfate, Ind. Eng. Chem. Res., 51 (2012) 13632–13638.
[26] D. Zhou, L. Chen, C. Zhang, Y. Yu, L. Zhang, F. Wu, A novel photochemical system of ferrous sulfite complex: kinetics and mechanisms of rapid decolorization of Acid Orange 7 in aqueous solutions, Water Res., 57 (2014) 87–95.
[27] L. Zhang, L. Chen, M. Xiao, L. Zhang, F. Wu, L. Ge, Enhanced decolorization of Orange II solutions by the Fe(II)–sulfite system under Xenon lamp irradiation, Ind. Eng. Chem. Res., 52 (2013) 10089–10094.
[28] Y. Guo, X. Lou, C. Fang, D. Xiao, Z. Wang, J. Liu, Novel photo-sulfite system: toward simultaneous transformations of inorganic and organic pollutants, Environ. Sci. Technol., 47 (2013) 11174–11181.
[29] P. Xie, Y. Guo, Y. Chen, Z. Wang, R. Shang, S. Wang, J. Ding, Y. Wan, W. Jiang, J. Ma, Application of a novel advanced oxidation

process using sulfite and zero-valent iron in treatment of organic pollutants, Chem. Eng. J., 314 (2017) 240–248.
[30] Z. Liu, S. Yang, Y. Yuan, J. Xu, Y. Zhu, J. Li, F. Wu, A novel heterogeneous system for sulfate radical generation through sulfite activation on a $CoFe_2O_4$ nanocatalyst surface, J. Hazard. Mater., 324 (2017) 583–592.
[31] D.C. Montgomery, Design and Analysis of Experiments, John Wiley & Sons, NY, 1997.
[32] A.R. Soleymani, J. Saien, S. Chin, H.A. Le, E. Park, J. Jurng, Modeling and optimization of a sono-assisted photocatalytic water treatment process via central composite design methodology, Process Saf. Environ. Prot., 94 (2015) 307–314.
[33] J. Saien, A.R. Soleymani, J.H. Sun, Parametric optimization of individual and hybridized AOPs of Fe^{2+}/H_2O_2 and $UV/S_2O_8^{2-}$ for rapid dye destruction in aqueous media, Desalination, 279 (2011) 298–305.
[34] D. Legrini, E. Oliveros, A.M. Braun, Photochemical processes for water treatment, Chem. Rev., 93 (1993) 671–696.
[35] A.R. Zarei, H. Rezaeivahidian, A.R. Soleymani, Investigation on removal of p-nitrophenol using a hybridized photo-thermal activated persulfate process: central composite design modeling, Process Saf. Environ. Prot., 98 (2015) 109–115.
[36] L.G. Devi, K.S.A. Raju, S.G. Kumar, K.E. Rajashekhar, Photo-degradation of di azo dye Bismarck Brown by advanced photo-Fenton process: influence of inorganic anions and evaluation of recycling efficiency of iron powder, J. Taiwan Inst. Chem. Eng., 42 (2011) 341–349.
[37] H.U. Farouk, A.A.A. Raman, W.M.A.W Daud, TiO_2 catalyst deactivation in textile wastewater treatment: current challenges and future advances, J. Ind. Eng. Chem., 33 (2016) 11–21.
[38] A. Rastogi, S.R. Al-Abed, D.D. Dionysiou, Sulfate radical-based ferrous-peroxymonosulfate oxidative system for PCBs degradation in aqueous and sediment systems, Appl. Catal., B, 85 (2009) 171–179.
[39] Y. Ding, L. Zhu, N. Wang, H. Tang, Sulfate radicals induced degradation of tetrabromobisphenol A with nanoscaled magnetic $CuFe_2O_4$ as a heterogeneous catalyst of peroxymonosulfate, Appl. Catal., B, 129 (2013) 153–162.
[40] C. Liang, H.-W. Su, Identification of sulfate and hydroxyl radicals in thermally activated persulfate, Ind. Eng. Chem. Res., 48 (2009) 5558–5562.
[41] X. Liu, T. Zang, Y. Zhou, L. Fang, Y. Shao, Degradation of sulfate atenolol by UV/peroxymonosulfate: kinetics effect of operational parameters and mechanism, Chemosphere, 93 (2013) 2717–2724.